The stabilization and the identification of the rockets' movement in vertical plane

Mihai Lungu

***Abstract*—**The paper presents some angular stabilization systems of the rockets in vertical pane using differential or integrator gyroscope. The first system has not a correction subsystem, while the second one has. One has determined the transfer functions (in closed loop or in open loop) of the two systems. The positioning of the systems' eigenvalues proofs the systems' stability. The systems respond very fast to a step input – the duration of the transient regime, for the two systems, is about one second. Using three different methods (least square method, instrumental variables' method - MVI and neural networks method), one makes the identification of the system. For both systems one obtains, using a Matlab/Simulink program, the frequency characteristics, indicial functions in the complex plane and in discrete plane, responses to impulse input in the complex and discrete planes. With least square method (LSM) the output of the system and the output of the model for the two systems were plotted. The identification is made very well – the two signals overlap. With the second identification method, one obtained the frequency characteristics for LSM and MVI on the same graphic. The identification is made using neural networks. Using this method, one obtained the indicial responses of the systems and of the neural networks (these signals overlap too), the weights and the biases of the neural networks and so on. The system's identification made also be done using the prediction error method (MEP). This method is more complicated than the others, but it is more precisely. The author also presents other two systems for rockets' stabilization: systems with accelerometer and correction subsystem (figures 16 and 17). These two systems also give good stabilization results.

***Keywords*—** rockets' movement, stabilization, identification methods, differentiator gyroscope, neural network.

I. Introduction

THE stabilization systems for the anti-aircraft rockets, air-to-air rockets and ground-air rockets fulfill the functions of control over the load. Since most of these oscillations damping is weak $(\xi \le 0{,}1)$, it is difficult to control the overload. The more the speed and flight altitude increases, the more difficult this mission is. Thus, the stabilization systems must correct the dynamic characteristics of the rockets. One also requires that the stabilization systems reduce the influence of external disturbances and internal noise. For this, bandwidth of the control and disturbance signals is chosen according to technical quality indicators [1].

The first part of this paper was published in the Proceedings of the International Conference on Circuits, Systems and Signals (IEEE.AM), Malta, September 15 – 17, 2010, pp. 51 – 56, ISSN: 1792-4324, ISBN: 978-960-474-226-4. After the conference, it received the recommendation to be extended and published by NAUN Journal.

Manuscript received September 30, 2010.

Mihai Lungu is Lecturer at the University of Craiova, Faculty of Electrical Engineering, Department of Avionics. 107, Decebal Blv., Craiova, Romania,

Email: Lma1312@yahoo.com, mlungu@elth.ucv.ro.

II. Dynamics of the rockets' movement

Next, one studies the stabilization systems' dynamics of rockets with cross empennage. Mathematical model of rocket's motion in the vertical plane is given by equations' system (1), the coefficients being those of form (2).

$$\begin{cases} \dot{\theta} = d_1\alpha + d_5\delta, \\ \dot{\omega}_z = d_3\alpha - d_2\delta - d_4\omega_z, \\ \dot{\theta} = \omega_z, \alpha = \theta - \vartheta, \end{cases} \tag{1}$$

where θ is the pitch angle of the rocket, ω_z – the pitch angular velocity, α – the incidence angle of the rocket, δ – the rocket's command, ϑ – the slope of the trajectory; the other terms are coefficients with formula [2]

$$d_1 = \frac{\rho\frac{V^2}{2}Sc_y^{\alpha} + F_T}{mV} = \frac{1}{T_V}, d_2 = \frac{\rho\frac{V^2}{2}SlC_z^{\delta}}{J_z}, \\ d_3 = \frac{\rho\frac{V^2}{2}SlC_z^{\alpha}}{J_z}, d_4 = \frac{\rho\frac{V^2}{2}Sl^2C_z^{\omega}}{J_z}, d_5 = \frac{\rho\frac{V^2}{2}Sc_y^{\delta}}{mV}. \tag{2}$$

To obtain the frequency characteristics, step and impulse responses and identification of the system using three different methods (least square method, instrumental variables' method and neural networks method), one uses the following coefficients

$$T_1 = \frac{1}{d_1} = T_V, T_2 = \frac{1}{\sqrt{d_1d_4 - d_3}}, \xi = \frac{1}{2}\frac{d_1 + d_4}{\sqrt{d_1d_4 - d_3}}, \\ k_{\theta} = \frac{d_1d_2}{d_1d_4 - d_3}, k_{\alpha} = \frac{d_2}{d_1d_4 - d_3}, k_W = k_{\theta}V. \tag{3}$$

In the case of vertical flight of the rockets, the above equations set suffers little modifications

$$T_1 = \frac{1}{d_1} = T_V, T_2 = \frac{1}{\sqrt{d_1 d_4 + d_3}}, \xi = \frac{1}{2}\frac{d_1 + d_4}{\sqrt{d_1 d_4 + d_3}},$$
$$k_\theta = \frac{d_1 d_2}{d_1 d_4 + d_3}, k_\alpha = \frac{d_2}{d_1 d_4 + d_3}, k_W = k_\theta V. \quad (4)$$

For each rocket's type one must obtain the variation in time of coefficients d_i, $i = \overline{1,5}$. In fig.1 the time variation curves of these coefficients for a ERLIKON rocket are presented. The values of these coefficients for second 10 of the flight are

$$d_1 = 1.125\left[1/s\right]; d_2 = 25\left[1/s^2\right]; d_3 = 14.285\left[1/s^2\right];$$
$$d_4 = 0.535\left[1/s\right]; k_\theta = 1.889\left[1/s\right]; \xi = 0.215; T_1 = 0.888. \quad (5)$$

The coefficients d_i characterize the stability of the system and the stability reserves; if $d_5 = 0$, then $n_v^\alpha = d_1$. The maneuverability of the system may be expressed on a graded scale which permits the choose of optimal maneuverability [1].

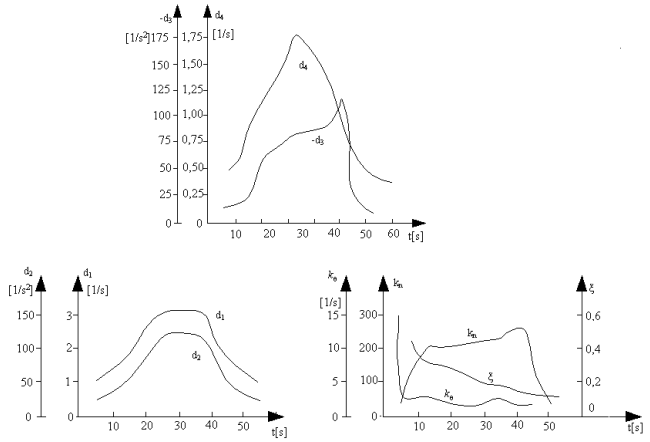

Fig.1 Time variation curves of the coefficients from rockets' dynamics equations

The maneuverability of the system depends on an indicator which expresses the dependence of the ratio T_2 / T_1 or of the product $n_v^\alpha T_2$ of the damp coefficient ξ. For the stability's improvement and maneuverability's increase one uses a negative feedback after angular velocity $\dot{\theta}$; it leads to the increase of the damp coefficient.

III. Angular Stabilization Systems with Differential Gyroscope, With or Without Correction Subsystem

The block diagram of the rockets' angular stabilization system with differential gyroscope, without correction subsystem is presented in fig.2. The input variable is the rocket's command u_v, while the output of the system is the pitch angle (θ) or the pitch angular velocity $(\dot{\theta})$; the differentiator gyroscope measures this angular velocity and gives a voltage signal which is applied to the input of the differential amplifier [1].

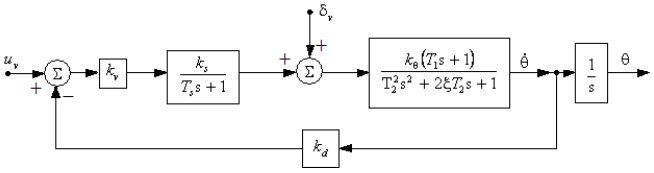

Fig.2 The block diagram of the rockets' angular stabilization system with differential gyroscope and without correction subsystem

For the system from fig.2, with negative unitary feedback, the closed loop transfer function and the open loop transfer function are, respectively

$$H_{u_V}^{\theta}(s) = \frac{\theta(s)}{u_V(s)} = \frac{\dfrac{k_v k_s k_\theta (T_1 s + 1)}{s(T_s s + 1)(T_2^2 s^2 + 2\xi T_2 s + 1)}}{1 + \dfrac{k_d k_v k_s k_\theta (T_1 s + 1)}{(T_s s + 1)(T_2^2 s^2 + 2\xi T_2 s + 1)}}; \quad (6)$$

$$H_{u_V}^{\theta}(s) = \frac{\theta(s)}{u_V(s)} = \frac{k_v k_s k_\theta (T_1 s + 1)}{C_4 s^4 + C_3 s^3 + C_2 s^2 + C_1 s},$$

$$H_d(s) = \frac{k_v k_s k_\theta (T_1 s + 1)}{C_4 s^4 + C_3 s^3 + C_2 s^2 + C_1' s + C_0'}, \quad (7)$$

where

$$C_1 = 1 + k_d k_v k_s k_\theta; C_2 = T_s + 2\xi T_2 + k_d k_v k_s k_\theta T_1;$$
$$C_3 = 2\xi T_2 T_s + T_2^2; C_4 = T_s T_2^2; \quad (8)$$
$$C_1' = 1 + k_d k_v k_s k_\theta - k_v k_s k_\theta T_1; C_0' = -k_v k_s k_\theta.$$

The block diagram of the rockets' angular stabilization system with differential gyroscope and with correction subsystem is presented in fig.3.

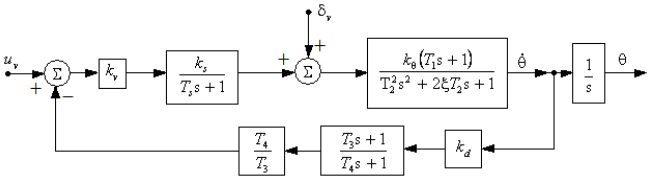

Fig.3 The block diagram of the rockets' angular stabilization system with differential gyroscope and correction subsystem

For the system from fig.3, with negative unitary feedback, the closed loop transfer function is

$$H_{u_v}^{\theta}(s) = \frac{\theta(s)}{u_v(s)} = \frac{\dfrac{k_v k_s k_\theta (T_1 s + 1)}{s(T_s s + 1)(T_2^2 s^2 + 2\xi T_2 s + 1)}}{1 + \dfrac{k_d k_v k_s k_\theta (T_1 s + 1)}{(T_s s + 1)(T_2^2 s^2 + 2\xi T_2 s + 1)} \cdot \dfrac{T_4}{T_3} \cdot \dfrac{T_3 s + 1}{T_4 s + 1}}; \quad (9)$$

$$H_{u_v}^{\theta}(s) = \frac{\theta(s)}{u_v(s)} = \frac{B_2 s^2 + B_1 s + B_0}{A_5 s^5 + A_4 s^4 + A_3 s^3 + A_2 s^2 + A_1 s},$$

where

$$B_2 = T_1T_4T_3k_vk_sk_\theta\ ;\ B_1 = T_3k_vk_sk_\theta(T_1+T_4);\ B_0 = T_3k_vk_sk_\theta\ ;$$
$$A_5 = T_3T_4T_sT_2^2\ ;\ A_4 = 2\xi T_2T_4T_3T_s + T_3T_2^2(T_4+T_s);$$
$$A_3 = T_3T_4T_s + 2\xi T_2T_3(T_4+T_s) + T_3T_2^2 + k_dk_vk_sk_\theta T_1T_3T_4\ ; \quad (10)$$
$$A_2 = T_3T_4 + T_sT_3 + 2\xi T_2T_3 + k_dk_vk_sk_\theta(T_1+T_3);$$
$$A_1 = T_3 + k_dk_vk_sk_\theta T_4\ .$$

The open loop transfer function for the system from fig.3, with negative unitary feedback is

$$H_d(s) = \frac{B_2s^2 + B_1s + B_0}{A_5s^5 + A_4s^4 + A_3s^3 + (A_2 - B_2)s^2 + (A_1 - B_1)s - B_0}. \quad (11)$$

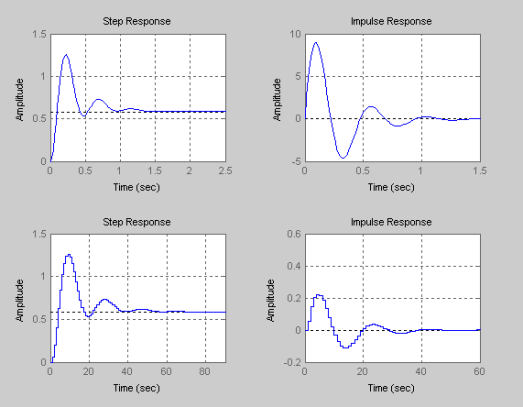

Fig.4 The indicial functions and responses to impulse input in the complex and discrete planes for the system from fig.2

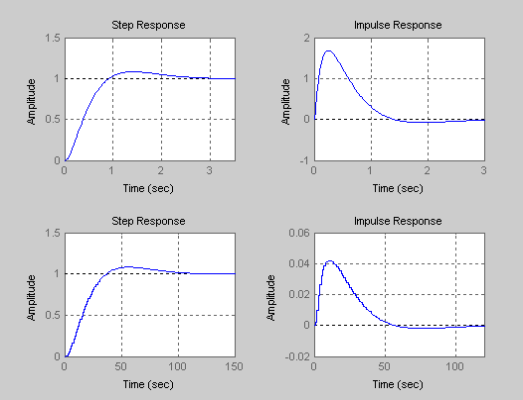

Fig.5 The indicial functions and responses to impulse input in the complex and discrete planes for the system from fig.3

For both systems one obtains, using a Matlab/Simulink program (see the Appendix), the frequency characteristics, indicial functions in the complex plane and in discrete plane, responses to impulse input in the complex and discrete planes. Also, one identifies the systems using three different methods (least square method, instrumental variables' method and neural networks method). For each of these methods, some graphics were obtained.

For the system without correction subsystem, the indicial functions and responses to impulse input in the complex and discrete planes are presented in fig.4 (the first two graphics correspond to the complex plane, while the last two correspond to the discrete plane). The program calculates the matrices that describe the state equations of the system in the complex plane or in the discrete plane. Also, the Matlab/Simulink program gives the transfer functions in complex description or in discrete description.

For the system with correction subsystem, one has obtained the graphic characteristics from fig.5.

IV. IDENTIFICATION OF THE SYSTEMS USING THE LEAST SQUARE METHOD (LSM)

A state estimator must assure the controllability of the system whose parameters are estimated, whatever the adaptive structure [2], [3]. The least square method doesn't always give models characterized by controllability. That's why in some cases it must be modified. The system, whose parameters must be determined, is described by the equation

$$L(z^{-1})y(t) = z^{-q}M(z^{-1})u(t) + C(z^{-1})e(t) + d, \quad (12)$$

where z^{-1} – the delay operator and the polynomials $L(z^{-1})$ and $M(z^{-1})$ are

$$L(z^{-1}) = 1 + a_1z^{-1} + a_2z^{-2} + ... + a_nz^{-n},$$
$$M(z^{-1}) = b_0 + b_1z^{-1} + b_2z^{-2} + ... + b_mz^{-m}; \quad (13)$$

The estimated model $\hat{A}$ of the leading system A (aircraft), obtained by an parametric identification method, may be described by equation

$$\hat{L}(z^{-1})y(t) = z^{-q}\hat{M}(z^{-1})u(t) + \hat{C}(z^{-1})\hat{e}(t) + d, \quad (14)$$

where $\hat{e}(t)$ is the noise applied to the model and the polynomials $\hat{L}(z^{-1}), \hat{M}(z^{-1})$ and $\hat{C}(z^{-1})$ have expressions

$$\hat{L}(z^{-1}) = 1 + \hat{a}_1z^{-1} + \hat{a}_2z^{-2} + ... + \hat{a}_nz^{-n},$$
$$\hat{M}(z^{-1}) = \hat{b}_0 + \hat{b}_1z^{-1} + \hat{b}_2z^{-2} + ... + \hat{b}_mz^{-m}, \quad (15)$$
$$\hat{C}(z^{-1}) = 1 + \hat{c}_1z^{-1} + \hat{c}_2z^{-2} + ... + \hat{c}_nz^{-n}.$$

LSM algorithm (least square algorithm) modification is based upon the discrete transfer function modification through origin pole $(z = 0)$ compensation. The modified LSM algorithm (LSMM) builds a convergent vector $v(t)$ and with it the vector of the estimated parameters [4]

$$\hat{b}'(k) = \hat{b}(k) + P(k)v(k). \quad (16)$$

Thus, the coefficient $\hat{b}'$ is almost non-null.

The control law may be chosen of general form

$$u(k) = R\left(z^{-1}, \hat{b}'\right)u(k) + S\left(z^{-1}, \hat{b}'\right)y(k), \tag{17}$$

with the polynomials

$$R\left(z^{-1}, \hat{b}'\right) = \sum_{i=1}^{\alpha} z^{-i} r_i(\hat{b}') \,, S\left(z^{-1}, \hat{b}'\right) = \sum_{i=0}^{\beta} z^{-i} s_i(\hat{b}'). \tag{18}$$

The closed loop system is described by equation [4]

$$W(k+1) = D\left(z^{-1}, \hat{b}'\right)W(k) + \begin{bmatrix} e(k+1) \\ 0 \end{bmatrix}, \tag{19}$$

where

$$D\left(z^{-1}, \hat{b}'\right) = \begin{bmatrix} z\left[1 - \hat{L}\left(z^{-1}, \hat{b}'\right)\right] & \hat{M}\left(z^{-1}, \hat{b}'\right) \\ zS\left(z^{-1}, \hat{b}'\right) & zR\left(z^{-1}, \hat{b}'\right) \end{bmatrix}, \tag{20}$$

and

$$e(k+1) = x^T(k)\left[b(k) - b^T(k)\right] + n(k+1), \tag{21}$$

$n(k+1)$ is a white noise.

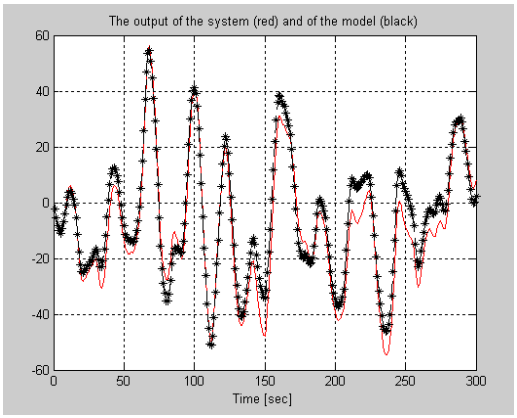

Fig.6 The output of the system and of the model for the system with differential gyroscope and without correction subsystem

In the Matlab program, one forms first the matrices A_q and B_q (they contain the coefficients of the discrete transfer function). The input u and the perturbation e of the leaded system are chosen as random type. For the $\hat{b}$ parameters of model $\hat{A}$ estimation one uses **ARX** operator from Matlab, which has the following syntax **th=ARX(z,nn),** where $\boldsymbol{z} = [y \; u]-$ matrix that contains the output vector (y) and the input vector (u); $\mathbf{nn} = [na \; nb \; nc]-$ defines the denominator order (na), numerator order (nb) and the model's delay (nc); **th** returns the estimated parameters in **theta** format (the elements of the vector $\hat{b}$) using the least square method. The program plots the characteristics $y(t)$ and $\hat{y}(t)$, presented in fig.6 and fig.7; $y(t)$ is the output of the control system (A), while $\hat{y}(t)$ is the output of the estimated model $(\hat{A})$.

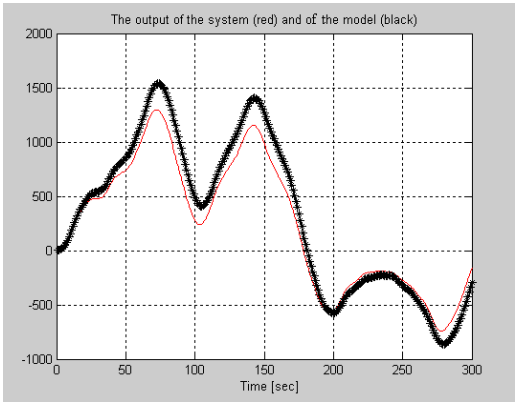

Fig.7 The output of the system and of the model for the system with differential gyroscope and correction subsystem

As one can see in the above figures that the identification is made very well - the two signals overlap $(\hat{y} \to y)$.

V. IDENTIFICATION OF THE SYSTEMS USING THE INSTRUMENTAL VARIABLES' METHOD (MVI)

This method is a generalization of LSM. It gives the estimated parameters only for the determinist part of the model $\hat{A}$ and not for the parameters of the polynomial $\hat{C}(z^{-1})$ associated to the random perturbation. The control system model (A) is described by the equation (12) and the one of the estimated model $(\hat{A})$ by equation (14); in this equation one considers $C(z^{-1}) = 1$. The equation equivalent to equation (14) is

$$y(k) = x^T(k)\hat{b} + \hat{e}(k). \tag{22}$$

By multiplication of this equation with $W(k)-$ instrumental variable vector (whose elements haven't physic significations, they are only necessary "instruments" for the $\hat{b}$ estimation), one obtains the equation of estimator $\hat{b}$

$$\sum_{k=1}^{N} W(k)y(k) \cong \left(\sum_{k=1}^{N} W(k)x^T(k)\right)\hat{b} \tag{23}$$

or

$$\hat{b} = \left[\sum_{k=1}^{N} W(k)x^T(k)\right]^{-1}\left[\sum_{k=1}^{N} W(k)y(k)\right], \tag{24}$$

where N is the measurements number; the vector W may be chosen in different ways. Let vector W be [5]

$$W(k) = F\left(z^{-1}\right)\left[u(k-1)\ u(k-2)\ \ldots\ u(k-n_W)\right]^T, \quad (25)$$

where $n_W = m + n$; if $\hat{L}\left(z^{-1}\right)$ and $\hat{M}\left(z^{-1}\right)$ are the $L\left(z^{-1}\right)$ and $M\left(z^{-1}\right)$ polynomials estimations, one chooses

$$F\left(z^{-1}\right) = \hat{L}^{-1}\left(z^{-1}\right). \quad (26)$$

The input u and perturbation e of the leading system are random type. For the parameters estimation of the vector $\hat{b}$ one uses, in Matlab, the operator **iv4**. In fig. 8 and fig.9 the frequency characteristics for the two systems (using LSM – continuous line, blue color and MVI – dashed line, red color) are plotted.

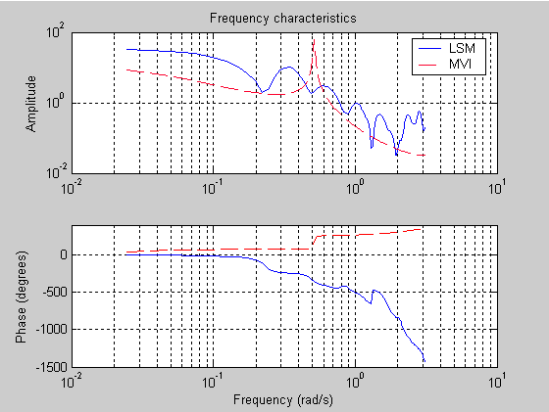

Fig.8 The frequency characteristics for the system with differential gyroscope and without correction subsystem

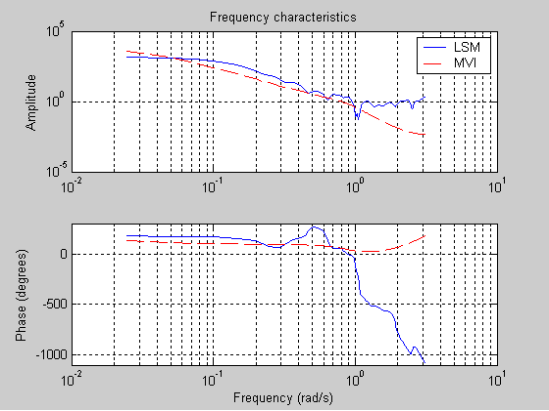

Fig.9 The frequency characteristics for the system with differential gyroscope and correction subsystem

VI. IDENTIFICATION OF THE SYSTEMS USING THE NEURAL NETWORKS' METHOD

Flying parameters' modification and atmospheric disturbances leads to difficulties in stability derivates calculus and to flying objects' models stabilization. That's why one may use identification methods or state estimate methods [6], [7], [8], [9], [10], [11]. The identification method presented in this paper is based on a neural network's use. As one can see in fig.10 [6], for off-line identification, a feed-forward neural network is used; the network is trained by minimizing the quadratic quality indicator $J(k) = \frac{1}{2}e^2(k), e(k)$ being the training error.

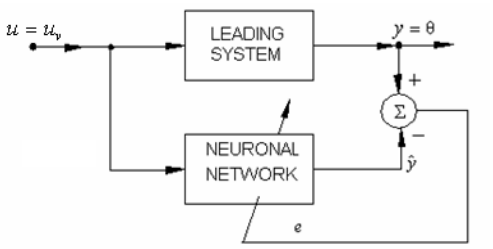

Fig.10. Dynamic model of the control system

The dynamic of the rockets' movement may be described by equation

$$y(k) = f\left(y(k-1)\,y(k-2)\cdots y(k-n_y)\ u(k-q)\cdots u(k-q-n_u+1)\right), \quad (27)$$

with $y = \theta$ – the pitch angle, $u = u_v$ – rocket's command, q – dead time; n_y and n_u express the system's order.

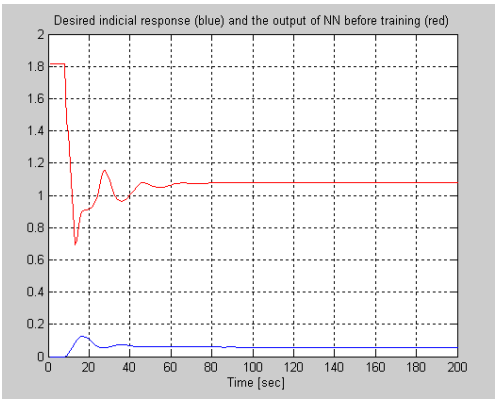

Fig.11 The output of the system from fig.2 (blue color) and the output of the NN (red color) before training.

If nothing is known about the control system (n_y, n_u, q, f and n_h – the number of hidden layer neurons), by identification one determines these parameters. So that, starting from minimal neural network's architecture (numbers n_u, n_h, n_y and q) and imposing a value for the error $e(k)$ and a maxim number of training epochs, the neural networks begins the training process. If the error $e(k)$ doesn't tend to the desired value then n_u, n_y and n_h are modified.

For identification process's simulation of the rockets' dynamics with neural network one may use discrete transfer

function associated to the two systems. A neural network with one hidden layer is chosen. This network is characterized by $n_u = 1, n_y = 3, n_h = 5$ and $q = 0$.

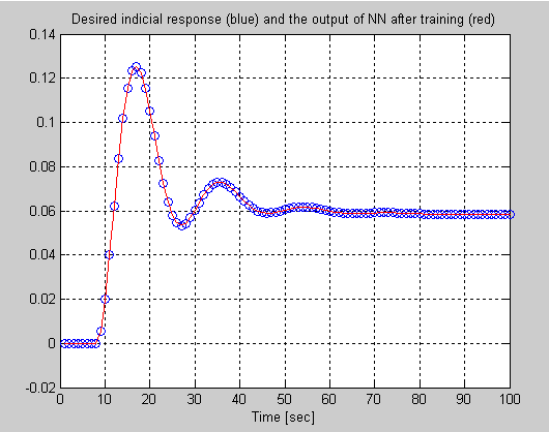

Fig.12 The output of the system from fig.2 (blue color) and the output of the NN (red color) after training.

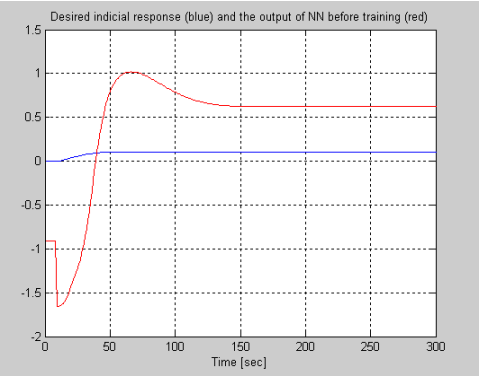

Fig.13 The output of the system from fig.3 (blue color) and the output of the NN (red color) before training.

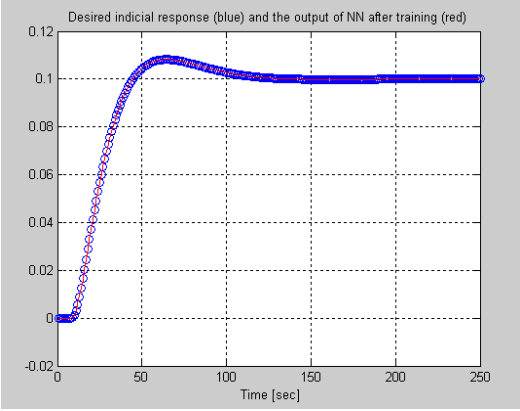

Fig.14 The output of the system from fig.3 (blue color) and the output of the NN (red color) after training.

One chooses calculus steps (p), which is equal with vector y's components number (the values at respective moments of the control system). The matrix of neural network P is obtained (it has the dimension $((n_u + n_y) \times (p-3))$. Also, matrix T (of desired output of the network, which represents control system's output values matrix) is the matrix of the system output's values at time moments corresponding calculus steps; $\dim(T) = n_e \times (p-3), n_e$ being output neurons' number (in this example $n_e = 1$).

In fig.11 one presents the output of the system from fig.2 (blue color) and the output of the NN (red color) before training. After the training process, the two signals overlap (fig.12). For the system with correction subsystem, the corresponding graphics are the ones from fig.13 and fig.14.

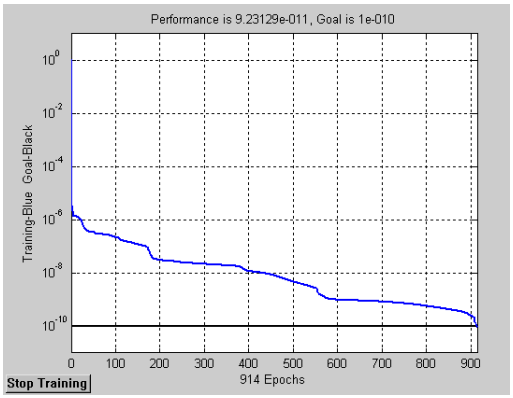

Fig.15 Dependence between error of the training process and training epochs' number for the system from fig.2

Neural network's training is made using instruction "train" till the moment when $e(k) = y(k) - \hat{y}(k) \to e_{\text{imposed}}(k)$ or until the number of training epochs is reached (in our example this number has been chosen 10000); $e_{\text{imposed}}(k) = 10^{-10}$ for the first system and $e_{\text{imposed}}(k) = 10^{-8}$ for the second one. In fig.15 (for the system from fig.2) and fig.16 (for the system from fig.3) the dependence between error $e(k)$ and training epochs' number is presented.

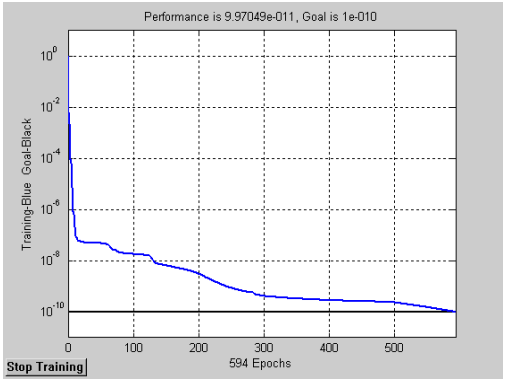

Fig.15 Dependence between error of the training process and training epochs' number for the system from fig.3

The training process takes longer in the case of first system compared with the second one because for the first system the desired error is greater then the second case desired error.

By neural network's training pseudo – neurons weight matrix W_1 and hidden layer neurons weight vector W_2 are obtained. Also, vectors B_1 and B_2, which contains polarization coefficients' values (bias) for neurons from hidden layer and for output neuron, respectively, are obtained. For the two systems they are, respectively

$$W_1 = \begin{bmatrix} 27.6429 & 16.0283 & 6.9687 & -7.4648 \\ -14.6652 & -2.0602 & 16.4490 & 31.9792 \\ 4.5626 & -14.8750 & 16.1572 & 22.4523 \\ -1.1713 & 26.1090 & 19.3306 & -9.2346 \\ 19.9705 & -3.1093 & -17.3665 & 25.1677 \end{bmatrix}; B_1 = \begin{bmatrix} -6.7037 \\ 1.2076 \\ -2.7673 \\ -4.1409 \\ -1.9235 \end{bmatrix}; \quad (28)$$

$$W_2 = \begin{bmatrix} -0.0033 & -0.5346 & 0.1737 & 0.0001 & 0.0031 \end{bmatrix}, B_2 = \begin{bmatrix} 0.6191 \end{bmatrix}$$

or

$$W_1 = \begin{bmatrix} -16.4718 & 13.4626 & 18.8918 & -28.3872 \\ 18.5041 & -9.7520 & 4.5062 & 34.9162 \\ -15.1027 & 28.5663 & -19.7417 & -8.5982 \\ -24.1919 & -2.7047 & 13.8729 & 28.8785 \\ -31.4477 & -5.2817 & 21.9340 & 0.1910 \end{bmatrix}; B_1 = \begin{bmatrix} 2.5634 \\ -3.4015 \\ 1.2514 \\ -1.6604 \\ -1.3155 \end{bmatrix}; \quad (29)$$

$$W_2 = \begin{bmatrix} 0.0327 & -0.0872 & -0.2229 & 0.0172 & -0.1027 \end{bmatrix}, B_2 = \begin{bmatrix} -0.0031 \end{bmatrix}.$$

VII. OTHER ROCKETS' STABILIZATION SYSTEMS

Stabilization system that uses differentiator gyroscope, although has superior dynamic performances, doesn't assure their constant in different flight regimes. That's why, this system is recommended only for the stabilization of the rockets' angular position. The mono-loop stabilization systems have some disadvantages which prevent their use for the overload's control. Much better are the bi-loop stabilization systems.

The block diagram of the rockets' angular stabilization system with differentiator gyroscope, accelerometer and correction subsystem is presented in figure 16 [1]. The input variable is the rocket's command u_v, while the output of the system is the rocket's overload n_v. On the direct way of the system one has introduced an integrator gyroscope and on the feedback of the exterior contour – an acceleration transducer (accelerometer), a correction network with the transfer function

$$H_c(s) = \frac{T_4'}{T_3'} \frac{T_3's + 1}{T_4's + 1} \quad (30)$$

and an amplifier with k_k amplification factor for the compensation of the voltage's failure at the output of the correction network (subsystem). The transfer function of the interior loop is calculated as follows [12],

$$H_i(s) = \frac{k_v \cdot \frac{k_s}{T_s s + 1} \cdot \frac{k_n}{T_2^2 s^2 + 2\xi T_2 s + 1}}{1 + \frac{57.3g}{V}(T_1 s + 1) \cdot \frac{T_4}{T_3} \cdot \frac{T_3 s + 1}{T_4 s + 1} \cdot k_d \cdot k_v \cdot \frac{k_s}{T_s s + 1} \cdot \frac{k_n}{T_2^2 s^2 + 2\xi T_2 s + 1}}. \quad (31)$$

The closed loop transfer function is obtained with equation

$$H_{u_v}^{n_v}(s) = \frac{n_v(s)}{u_v(s)} = k_u \cdot \frac{H_i(s)}{1 + k_k \cdot \frac{T_4'}{T_3'} \cdot \frac{T_3's + 1}{T_4's + 1} \cdot k_a \cdot H_i(s)}. \quad (32)$$

After calculus, the transfer function in closed loop becomes

$$H_0(s) = \frac{n_v(s)}{u_v(s)} = \frac{B_2 s^2 + B_1 s + B_0}{A_5 s^5 + A_4 s^4 + A_3 s^3 + A_2 s^2 + A_1 s + A_0}; \quad (33)$$

the transfer function in open loop is calculated in rapport with the one presented above. The coefficients that appear in the numerator and dominator of the transfer function (33) are

$$\begin{aligned}
&B_2 = k_u k_v k_s k_n V T_3 T_3' T_4 T_4'; B_1 = k_u k_v k_s k_n V T_3 T_3' \cdot (T_4 + T_4'); \\
&B_0 = k_u k_v k_s k_n V T_3 T_3'; \\
&A_5 = T_3 T_3' V T_s T_4 T_4' T_s T_2^2; \\
&A_4 = T_3 T_3' V \left(T_2^2 T_4 T_4' + 2\xi T_2 T_s T_4 T_4' V\right) + T_3 T_3' V \left[T_s T_2^2 (T_4 + T_4')\right]; \\
&A_3 = T_3 T_3' V \left[2\xi T_2 T_4 T_4' + T_s T_4 T_4' + T_2^2 (T_4 + T_4')\right] + \\
&+ T_3 T_3' V \left[T_s T_2^2 + 2\xi T_s T_2 (T_4 + T_4')\right] + 57.3 g k_v k_s k_n k_d T_4 T_3' (T_1 T_3 + T_4'); \\
&A_2 = T_3 T_3' V \left[T_4 T_4' + 2\xi T_2 (T_4 + T_4') + T_s (T_4 + T_4') + T_2^2 + 2\xi T_s T_2\right] + \\
&+ 57.3 g k_v k_s k_n k_d T_4 T_3' (T_1 T_4' + T_1 T_3 + T_3 T_4') + k_a k_k k_v k_s k_n T_3 T_4' V T_3' T_4; \\
&A_1 = T_3 T_3' V (T_4 + T_4' + 2\xi T_2 + T_s) + + k_a k_k k_v k_s k_n T_3 T_4' V (T_3' + T_4') + \\
&+ 57.3 g k_v k_s k_n k_d T_4 T_3' (T_4' + T_1 + T_3); \\
&A_0 = T_3 T_3' V + 57.3 g k_v k_s k_n k_d T_4 T_3' + k_a k_k k_v k_s k_n T_3 T_4' V.
\end{aligned} \quad (34)$$

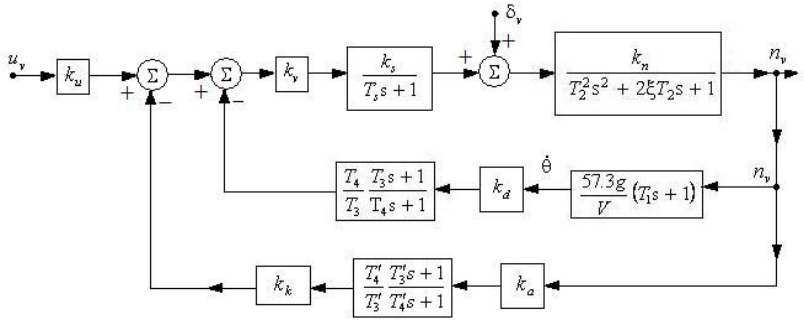

Fig.16: Block diagram of the rockets' angular stabilization system with differentiator gyroscope, accelerometer and correction subsystem

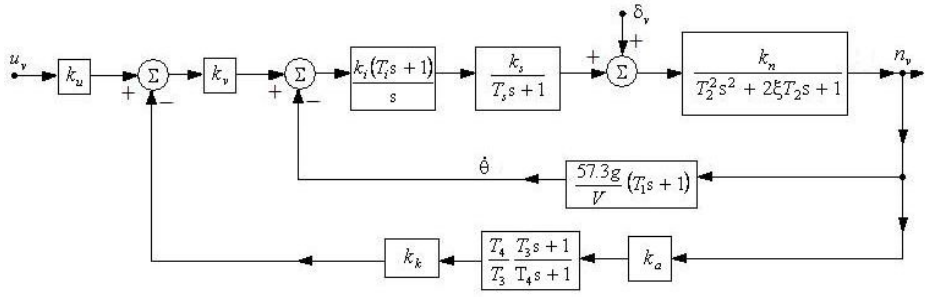

Fig.17: The block diagram of the rockets' angular stabilization system with integrator gyroscope, accelerometer and correction subsystem

The block diagram of the rockets' angular stabilization system with integrator gyroscope, accelerometer and correction subsystem is presented in figure 17 [1]. The input and the output variables are the same with the ones from the previous case.

On the direct way of the system one has introduced an integrator gyroscope and on the feedback of the exterior contour – an acceleration transducer (accelerometer), a correction network with the transfer function

$$H_c(\mathrm{s}) = \frac{T_4}{T_3}\frac{T_3\mathrm{s}+1}{T_4\mathrm{s}+1} \tag{35}$$

and an amplifier with k_k amplification factor for the compensation of the voltage's failure at the output of the correction network (subsystem). The transfer function of the interior loop is calculated as follows

$$H_i(\mathrm{s}) = \frac{\frac{k_i(T_i\mathrm{s}+1)}{\mathrm{s}}\cdot\frac{k_s}{T_s\mathrm{s}+1}\cdot\frac{k_n}{T_2^2\mathrm{s}^2+2\xi T_2\mathrm{s}+1}}{1+\frac{57.3\mathrm{g}}{\mathrm{V}}(T_1\mathrm{s}+1)\frac{K_i(T_i\mathrm{s}+1)}{\mathrm{s}}\cdot\frac{k_s}{T_s\mathrm{s}+1}\cdot\frac{k_n}{T_2^2\mathrm{s}^2+2\xi T_2\mathrm{s}+1}}. \tag{36}$$

The closed loop transfer function is obtained with equation

$$H_{u_v}^{n_v}(\mathrm{s}) = \frac{n_v(\mathrm{s})}{u_v(\mathrm{s})} = k_u\cdot\frac{k_v\cdot H_i(\mathrm{s})}{1+k_k\cdot\frac{T_4}{T_3}\cdot\frac{T_3\mathrm{s}+1}{\mathrm{T_4s}+1}\cdot k_a\cdot H_i(\mathrm{s})}. \tag{37}$$

In equations (36) and (37) the values of the constants are the ones from equation (33). After calculus, the transfer function in closed loop becomes

$$H_0(\mathrm{s}) = \frac{n_v(\mathrm{s})}{u_v(\mathrm{s})} = \frac{B_2\mathrm{s}^2+B_1\mathrm{s}+B_0}{A_5\mathrm{s}^5+A_4\mathrm{s}^4+A_3\mathrm{s}^3+A_2\mathrm{s}^2+A_1\mathrm{s}+A_0}; \tag{38}$$

the transfer function in open loop is calculated in rapport with the one presented above. The coefficients that appear in the numerator and dominator of the transfer function (38) are

$$\begin{aligned}
&B_2 = k_u k_v k_i k_s k_n T_3 T_4 T_i\ ;\ B_1 = k_u k_v k_i k_s k_n T_3\cdot(T_4+T_i);\\
&B_0 = k_u k_v k_i k_s k_n T_3\ ;\\
&A_5 = T_3 T_4 V T_s T_2^2\ ;\ A_4 = 2\xi T_3 T_s T_4 V + T_3 V T_2^2(T_3+T_4);\\
&A_3 = T_3 T_s T_4 V + T_3 V(T_s+T_4)\cdot 2\xi T_2 + T_3 V T_2^2 +\\
&\quad + 57.3 g T_3 T_1 T_4 k_i k_s k_n T_i\ ;\\
&A_2 = T_3 V(T_s+T_4) + T_3 V\cdot 2\xi T_2 + 57.3 g T_3 T_1 T_4 k_i k_s k_n T_i +\\
&\quad + k_i k_s k_n T_i\cdot 57.3 g T_3(T_1+T_4) + k_k k_a k_i k_s k_n T_4 V T_3 T_i\ ;\\
&A_1 = T_3 V + 57.3 g T_3(T_1+T_4) k_i k_s k_n + 57.3 g T_3 k_i k_s k_n T_i +\\
&\quad + k_k k_a k_i k_s k_n T_4 V(T_i+T_3);\\
&A_0 = 57.3 g T_3 k_i k_s k_n + k_k k_a k_i k_s k_n T_4 V\ .
\end{aligned} \tag{39}$$

VIII. IDENTIFICATION OF THE SYSTEM USING THE PREDICTION ERROR METHOD

The system's identification made also be done using the prediction error method. This method is more complicated than the others, but it is more precisely. MEP calculates the coefficients of the polynomials $M(\mathrm{z}^{-1}), L(\mathrm{z}^{-1})$ and the coefficients of the polynomials that "modify" perturbation which affects the leading system. Starting from an initial estimation, one calculates the parameter of the system through successive iterations till the convergence criteria is reached. The initial estimations used by MEP may be obtained using one of the previous methods [5], [13], [14], [15].

The prediction error is the perturbation e

$$e = y - \hat{y}. \tag{40}$$

The leading system is described by equation

$$L(\mathrm{z}^{-1})y = M(\mathrm{z}^{-1})u + C(\mathrm{z}^{-1})e. \tag{41}$$

Thus, the residue is

$$e = \frac{1}{C(\mathrm{z}^{-1})}\left[L(\mathrm{z}^{-1})y - M(\mathrm{z}^{-1})u\right] \tag{42}$$

The estimated parameters (the vector $\hat{b}$) are determined through the sum's minimization of the square prediction

errors

$$\hat{b} = \arg\left(\min_{b} \sum_{k=1}^{N} e^2(k) \right), \tag{43}$$

where N is the available data number. An estimation algorithm is the following one [5]:

1) one makes an initial estimation of the coefficients of $C(z^{-1})$ using a CMMP type method, and thus it results $\hat{C}(z^{-1})$;

2) using the previous estimation $(\hat{C})$, one calculates the filtering signals

$$\begin{aligned} u_f &= \hat{C}(z^{-1})u, \\ y_f &= \hat{C}(z^{-1})y; \end{aligned} \tag{44}$$

3) one determines the estimations $\hat{L}(z^{-1})$ and $\hat{M}(z^{-1})$ of the polynomials $L(z^{-1})$ and $M(z^{-1})$

$$\begin{aligned} \hat{L}(z^{-1}), \hat{M}(z^{-1}) &= \arg\left(\min_{L,M} \sum_{k=1}^{n} e^2(k) \Big|_{C=\hat{C}} \right) = \\ &= \arg\left[\min_{L,M} \sum_{i=1}^{N} \left(L(z^{-1})y_f - M(z^{-1})U_f \right)^2 \right]; \end{aligned} \tag{45}$$

4) hereby a new estimation $\hat{C}(z^{-1})$ is calculated [3]

$$C(z^{-1}) = \arg\left[\min_{C} \sum_{k=1}^{N} \left(\frac{1}{C(z^{-1})} \hat{V} \right)^2 \right], \tag{46}$$

where $\hat{V}$ is expressed function of assessments $\hat{L}(z^{-1})$ and $\hat{M}(z^{-1})$ from previous step;

$$\hat{V} = \hat{L}(z^{-1})y - M(z^{-1})u. \tag{47}$$

The calculus formula for $\hat{b}$ is

$$\hat{b} = \left[\sum_{k=1}^{N} x^F(k)\left(x^F(k)\right)^T \right]^{-1} \left[\sum_{k=1}^{N} x^T(k) y^F(k) \right]. \tag{48}$$

IX. CONCLUSIONS

The paper presents two angular stabilization systems of the rockets in vertical pane using differential gyroscope. The first system has not a correction subsystem, while the second one has. One has determined the transfer functions (in closed loop or in open loop) of the two systems; a study of stability is made. All the eigenvalues of the systems are placed in the left complex semi-plane. This is a proof of systems' stability. The systems respond very fast to a step input – the duration of the transient regimes is about one second. Using three different methods (least square method, instrumental variables' method and neural networks method), one makes the identification of the system. For both systems one obtains, using a Matlab/ Simulink program (the one from Appendix), the frequency characteristics, indicial functions in the complex plane and in discrete plane, responses to impulse input in the complex and discrete planes. With the least square method (LSM) the output of the system and the output of the model for the two systems are plotted (fig.6 and fig7). As one can see in these figures, the identification is made very well - the two signals overlap $(\hat{y} \to y)$.

With the second identification method (instrumental variables method - MVI), one obtained the frequency characteristics for LSM and MVI on the same graphic.

The identification may also be made using neural networks. Using this method, one obtained the indicial responses of the systems and of the neural networks (these signals overlap too), the weights and the biases of the neural networks and so on. One also presented the dependence between the error of the training process and the training epochs number for the two systems. The training process lasts longer in the case of first system (900 epochs) compared with the second one (600 epochs). This doesn't mean that the second system is better. This fact happens because for the first system the desired error is greater then the desired error in the second case.

APPENDIX

```
% Angular stabilization of the rocket in vertical plane
clear all;close all;
% The coefficients
d1=1.5;d2=37.5;d3=-18.75;d4=0.90;T1=0.66;T2=0.22;
Kteta=2.79;Kv=0.5;Kd=1;Ks=1;Ts=0.1;csi=0.05;Ks=1;
% The transfer functions
numi=[0 0 Kv*Ks*Kteta*T1 Kv*Ks*Kteta];
deni(1)= Ts*T2*T2;
deni(2)= Ts*2*eps*T2+T2*T2;
deni(3)= Ts+2*eps*T2+Kv*Kd*Ks*Kteta*T1;
deni(4)=1+Kd*Kv*Ks*Kteta;
deni=[deni(1) deni(2) deni(3) deni(4)];
numd=numi;dend=deni-numi;
sysi=tf(numi,deni);sysd=tf(numd,dend);
poli=pole(sysi);zerouri=zero(sysi);
[A,B,C,D]=tf2ss(numi,deni)
Ts=.025;sys_z=c2d(sysi,Ts);
[num_z,den_z]=tfdata(sys_z,'v');
sys_z=tf(num_z,den_z)
[A_z,B_z,C_z,D_z]=tf2ss(num_z,den_z); L=eig(A_z);
% Graphical characteristics
h=figure;margin(sysd);
[Gm,Pm,Wcg,Wcp]=margin(sysd)
Gm=20*log10(Gm); h=figure;
```

```
subplot(2,2,1);step(sysi);grid;
subplot(2,2,2);impulse(sysi);grid;
subplot(2,2,3);dstep(num_z,den_z);grid;
subplot(2,2,4);dimpulse(num_z,den_z);grid;
% System's identification using LSM
Bq=[num_z(2) num_z(3) num_z(4)];
Aq=[den_z(1) den_z(2) den_z(3) den_z(4)];
tho=poly2th(Aq,Bq); u=idinput(300,'rbs');
e=randn(300,1);y=idsim([u,e],tho);
z=[y,u]; nn=[3 2 0];th=ARX(z,nn);
y_model=idsim([u,e],th);
% Comparative graphics of the two systems
h=figure;tt=1:length(y);
plot(tt,y,'r',tt,y_model,'--*k');grid;
present(tho)
present(th)
% System's identification using MVI method
tho=poly2th(Aq,Bq); u=idinput(300,'rbs');
e=randn(300,1); y=idsim([u,e],tho);
z=[y,u]; nn=[3 2 0];th=iv4(z,nn);
% Frequency characteristics for LSM and MVI methods
h=figure;[Gs,Nss]=spa(z);
Gi=trf(th);bodeplot([Gs Gi]);grid;
present(tho)
present(th)
% System's identification using neural networks method
sim('S1');
sim('S2');
M=length(y);
ny=3;nu=1;nh=5;d=0;
% The obtaining of the matrix P
s1=max(0,nu+d-ny);s2=max(0,ny-nu-d);
s3=max(nu+d,ny);
P=uy(s1+1:M-ny,1)';        % P=uy(1:M-3,1)';
for i=2:ny
   P=[P;uy(s1+i:M-ny+i-1,1)'];
   % P=[P;uy(2:M-2,1)'];P=[P;uy(3:M-1,1)'];
end
for i=1:nu
  P=[P;uy(s2+i:M-d-nu+i-1,2)'];
  %P=[P;uy(3:M-1,2)'];
end
% The desired output of the system, t, is plotted
T=y(s3+1:M,1)'; timp=1:length(T);
h=figure;plot(timp,T,'k');grid;
% NN's initialization
Z=[min(P(1,:)) max(P(1,:));
  min(P(2,:)) max(P(2,:));
  min(P(3,:)) max(P(3,:));
  min(P(4,:)) max(P(4,:))];
h=figure;
net=newff(Z,[5 1],{'tansig' 'purelin'});
y1=sim(net,P);
% y1 is the output of the NN before training
plot(timp,T,'b',timp,y1,'r');grid; title('Desired indicial response
(blue) and the output of NN before training (red)');
xlabel ('Time [s]');
% NN's training
net.trainParam.epochs=10000;net.trainParam.goal=1e-10;
net = train(net,P,T);grid;
h=figure;y2 = sim(net,P);
% y2 is the output of the NN bafter training
plot(timp,T,'bo',timp,y2,'r');grid;
title('Desired indicial response (blue) and the output of NN
after training (red)'); xlabel('Time [sec]');
% Bias and weight calculus
W1=net.iw{1,1}
W2=net.lw{2,1}
B1=net.b{1}
B2=net.b{2}
```


ACKNOWLEDGMENT

This work was supported by the strategic grant POSDRU/89/1.5/S/61968 (2009), co-financed by the European Social Fund within the Sectorial Operational Program Human Resources Development 2007 - 2013.

REFERENCES

[1] I. Aron, R. Lungu "Automate de stabilizare si dirijare", Military Publisher, Bucharest, 1991.

[2] C. Teisanu, M. Calbureanu, "Sintering parameters influences on the iron base self-lubricating bearing porosity", Proceedings of the I*nternational Conference on Materials Science and Engineering Bramat 2003*, Brasov, vol. I, pp. 158-163.

[3] G. Stanescu, D. Bolcu, M. Calbureanu and others, "Determination of the thermal conductivity coefficient for the composite materials", *Mashinintelekt,* no. 12/2004, pp 13-16.

[4] D. Teodorescu, "Modele stohastice optimizate". Romania Academy Publisher, Bucharest, 1982.

[5] M. Tertisco, P. Stoica, Th. Popescu, "Identificarea asistata de calculator a sistemelor". Technical Publisher, 1987.

[6] M. Donald, "Automatic Flight Control Systems". New York – London – Sidney – Tokyo – Singapore, 1990.

[7] M.C. Campi, "The Problem of Pole-Zero Cancellation in Transfer Function Identification and Application to Adaptive Stabilization". *Automatica*, Vol. 32, no. 6, pp. 849-857, 1996.

[8] L. Ljung, J. Sjoberg, H. Hjalmarsson, "Identification, Adaptation, Learning – The Science of Learning Models from Data", Edited by S. Bittani, G, Picci, Springer Verlag Berlin Heidelberg, 1996.

[9] R. Lungu, "Automatizarea aparatelor de zbor". Universitaria Publisher, Craiova, 2002.

[10] K.S. Narendra, J. Balakrisman, "Adaptation and Learning Using Multiple Models Switching and Tuning". *IEEE. Control Systems*, 1995.

[11] K.S. Narendra, K. Parthasaranthy, "Identification and Control of dynamical systems using neural networks". *IEEE Transaction Neural Networks*, Vol.1, pp. 4-27, 1990.

[12] Lungu, M., Lungu, R., Bacanu, Gh. "Angular stabilization systems of the rockets in vertical plane using differentiator gyroscope". Recent Advances in Circuits, Systems and Signals, pp. 51 – 56. IEEE.AM International Conference on Circuits, Systems and Signals, Malta, September 15 – 17, 2010.

[13] Chelaru T.V., Pana V. "Stability and Control of the UAV Formations Flight". *WSEAS Transactions on systems and Control,* Issue 1, vol. 5, January 2010.

[14] Yasemin I. "Pitch Rate Damping of an Aircraft by Fuzzy and Classical PD Controller". *WSEAS Transactions on Systems and Control,* Issue 7, vol. 5, July 2010.

[15] Chelaru T.V., Pana V., Chelaru A. " Dynamic and Flight Control of the UAV formations". *WSEAS Transactions on Systems and Control,* Issue 4, vol. 4, April 2010.